

Measurements of Photon Plus Heavy Flavor Jet Cross Sections

D. Duggan (for the DØ Collaboration)
 Florida State University, Tallahassee, FL 32306, USA

Measurements of differential photon +c jet and photon +b jet production cross sections are presented using approximately 1 fb^{-1} of data collected by the DØ detector at the Tevatron $p\bar{p}$ collider at a center-of-mass energy of 1.96 TeV. Isolated photons are selected in the rapidity range $|y^\gamma| < 1.0$ and jets selected with rapidities $|y^{\text{jet}}| < 0.8$. The measurements are compared to next-to-leading order theoretical predictions.

1. INTRODUCTION

We present first preliminary measurements of differential $\gamma + c$ jet and $\gamma + b$ jet cross sections using $\sim 1 \text{ fb}^{-1}$ of data. These measurements were performed at the Fermilab Tevatron $p\bar{p}$ collider at $\sqrt{s} = 1.96 \text{ TeV}$ collected using the DØ detector. These measurements are differential with respect to the transverse momentum of the leading photon (p_T^γ), the rapidity of the leading jet (y^{jet}) and of the leading photon (y^γ). The results are presented in five p_T^γ bins and in two regions of photon–jet rapidities: $y^\gamma \cdot y^{\text{jet}} > 0$ (region 1) and $y^{\text{jet}} \cdot y^\gamma < 0$ (region 2).

2. DATA SELECTION

Events are recorded using the DØ detector [1] and must contain at least one photon candidate and at least one heavy flavor jet candidate. Both the chosen photon and jet candidates are required to be leading with respect to their p_T . The photon candidate p_T must be greater than 30 GeV, be located within the central calorimeter and have $|y^\gamma| < 1.0$. The leading jet must have $p_T > 15 \text{ GeV}$ and $|y^{\text{jet}}| < 0.8$. Additionally, events must also contain a primary vertex within 50 cm of the detector’s center along the beam pipe. This vertex is required to have at least three associated tracks, one with $p_T > 1.0 \text{ GeV}$ and a second with $p_T > 0.5 \text{ GeV}$. To suppress events containing cosmic muons and W bosons, the missing transverse energy (E_T^{Miss}) must pass the condition $E_T^{\text{Miss}} < 0.7 \cdot p_T^\gamma$.

Events are triggered using electromagnetic (EM) clusters consistent with photon shower profiles. The final photon energy is taken as the energy of the cluster within a cone of radius $R = 0.2$. An isolation requirement is imposed on the candidate photon such that the total energy in a cone of $R = 0.4$, excluding E_{EM} , must be less than 7% of E_{EM} . The cluster must also have a probability less than 0.1% to be spatially matched to any track in the event. The cluster’s transverse profile in the third layer of the EM calorimeter must be consistent with that of a photon. The primary vertex is further constrained to be within 10 cm of the most probable origin of the photon candidate along the beam pipe. To further suppress backgrounds coming from jets, an artificial neural network (ANN) [2], which uses additional single variable discriminants, was employed with the requirement of $\text{ANN} > 0.7$.

The energy of the leading jet is determined using DØ’s RunII jet reconstruction algorithm [3] with a cone of radius $R = 0.5$. Heavy flavor jets are identified using their long lifetimes by reconstructing displaced secondary vertices from the jet’s tracks. To best enhance the fraction of jets originating from heavy flavor quarks, an artificial neural network (bANN) was implemented. The bANN [4] uses variables characteristic of heavy flavor jets as inputs, trained such that the output of b jets tends toward one and that of light (udsg) jets tends to zero. For this selection, we require the bANN output > 0.85 .

3. PURITY ESTIMATES

To estimate the fraction of photons in the final data sample, the photon ANN output in data is fit with a template from signal photon Monte Carlo (MC) PYTHIA [5] simulation and a background dijet MC template. The fit is

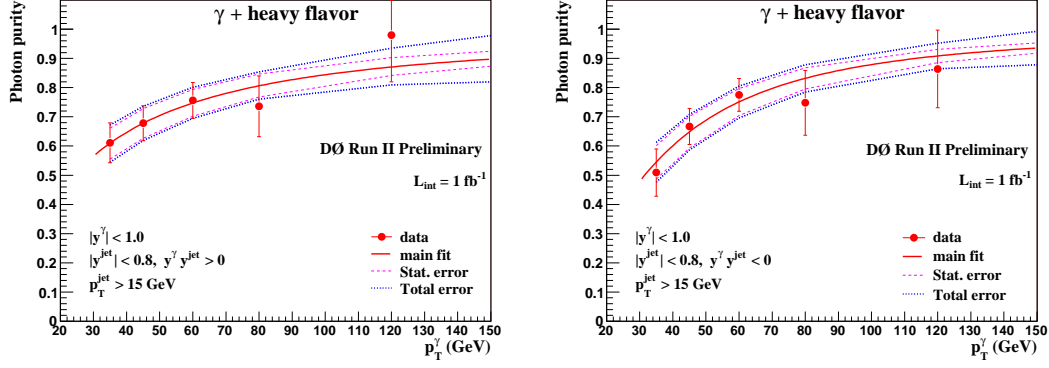


Figure 1: The photon purity in the selected $\gamma +$ heavy flavor jet events as a function of p_T^γ for both rapidity regions 1 (left) and 2 (right). The result of the $(1 - \exp(a + bp_T^\gamma))$ functional fit is shown by the full lines, together with the statistical uncertainty in the default fit (dashed lines) and the total uncertainty (dotted lines).

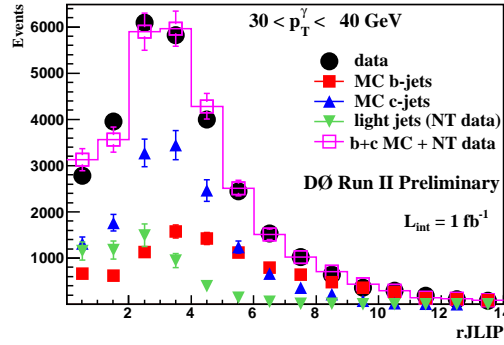


Figure 2: Distribution of the number of events in data for $P_{b\text{-jet}}$ after all selection criteria in the p_T^γ interval 30 to 40 GeV. The b , c and light jet template distributions are also shown normalized to their fitted fraction. The error bars on the data points show the combined statistical uncertainty from the data statistics and the flavor fraction fit.

performed in each p_T^γ bin and in each photon-jet rapidity region separately. The fit results are shown in Fig. 1.

To estimate the fraction of c and b jets in the final data sample, a different discriminant was used. It is defined as $P_{b\text{-jet}} = -\ln \prod_i P_{\text{track}}^i$, where P_{track}^i is the probability of a track in the jet cone to originate from the primary vertex, omitting the track with the lowest probability. $P_{b\text{-jet}}$ has large values for b jets and values closer to zero for light jets. A fit to the data $P_{b\text{-jet}}$ distribution is performed using MC templates for b and c jets, and the light jet template is taken from a light jet enriched data sample. The fit done in each p_T^γ bin, and to verify the quality of the fit, a combined flavor template is compared to the data as shown in Fig. 2.

4. CROSS SECTION RESULTS

The differential cross sections are presented in five p_T^γ bins and two regions of $y^\gamma \cdot y^{\text{jet}}$, corrected for p_T^γ smearing effects due to the finite resolution of the calorimeter using the unfolding method described in [6]. The measured cross sections are shown in Fig. 3 for $\gamma + b$ and $\gamma + c$ processes. Statistical uncertainties on the results vary from 0.2% in the lowest p_T^γ bin to 8–9% in the highest bin, while systematic uncertainties vary between 15–25%. The theoretical predictions from next-to-leading (NLO) order calculations are presented in Fig. 3 with the renormalization, factorization and fragmentation scales μ_R , μ_F , and μ_f set to p_T^γ . These predictions are preliminary [7] and are based

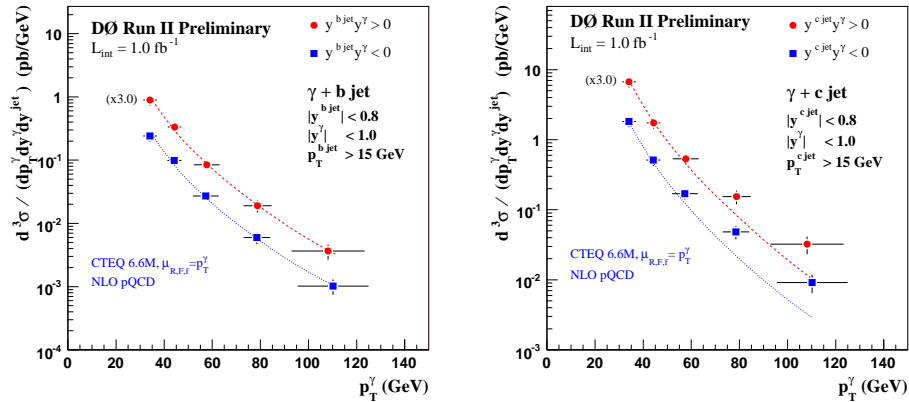


Figure 3: The $\gamma + b$ (left) and $\gamma + c$ (right) cross sections as a function of p_T^γ in regions 1 and 2. The uncertainties on the points in data are the full uncertainties. The NLO theoretical predictions using the CTEQ6.6M PDF set are shown by the dotted lines.

on techniques to calculate the analytic cross sections published in Ref. [8].

The ratios of the measured and predicted cross sections for both $\gamma + b$ and $\gamma + c$ cross sections in the two rapidity regions are shown in Fig. 4. The uncertainty due to the scale choice is estimated by simultaneously varying all three scales by a factor of two, $\mu_{R,F,f} = 0.5p_T^\gamma$, and $\mu_{R,F,f} = 2p_T^\gamma$. The theoretical predictions utilize the CTEQ6.6M PDF set with uncertainties calculated according to the prescription in [9].

Acknowledgments

The author is grateful to Tzvetalina Stavreva and Jeff Owens and thanks the staffs at Fermilab and collaborating institutions.

References

- [1] D0 Collaboration, V.M. Abazov *et al*, Nucl. Instrum. Methods A **565**, 463 (2006).
- [2] D0 Collaboration, V. Abazov *et al.*, Phys. Lett. B **666**, 435 (2008).
- [3] G.C. Blazey *et al.*, arXiv:hep-ex/0005012 (2000).
- [4] T. Scanlon, Ph.D. thesis, FERMILAB-THESIS-2006-43.
- [5] T. Sjostrand, Comp. Phys. Comm. **82**, 74 (1995).
- [6] B. Abbott *et al* (D0 Collaboration), Phys. Rev. D **64**, 032003 (2001).
- [7] T. Stavreva, J.F. Owens, “Photon + Heavy Flavor Cross Sections” (*in preparation*), 2008.
- [8] B.W. Harris, J.F. Owens, “The two cutoff phase space slicing method”, arXiv:hep-ph/0102128v2.
- [9] J. Pumplin *et al.*, J. High Energy Phys. **0207**, 12 (2002); D. Stump *et al.*, J. High Energy Phys. **0310**, 046 (2003).

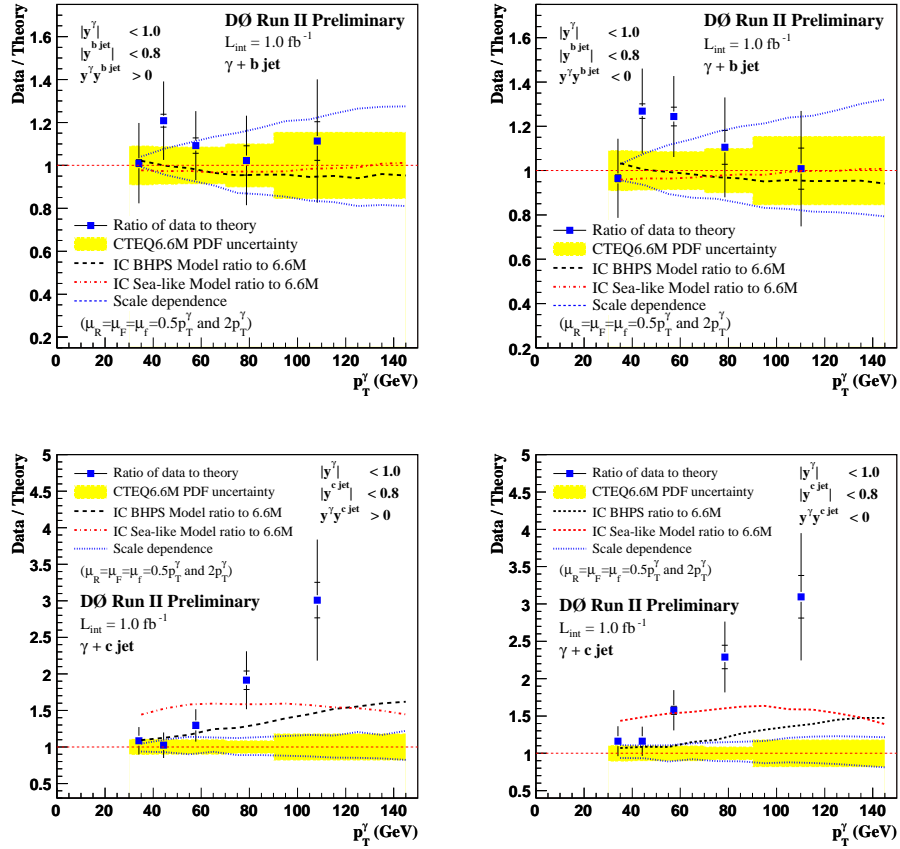


Figure 4: The $\gamma + b$ cross section ratio of data to theory as a function of p_T^γ in region 1 (top left) and region 2 (top right) and the $\gamma + c$ cross sections in region 1 (bottom left) and region 2 (bottom right). The uncertainties on the data points include both statistical (inner line) and full uncertainties (entire error bar) Also shown are the theoretical scale uncertainties and the CTEQ6.6M PDF uncertainties. The ratio of the central CTEQ6.6M prediction to two *intrinsic charm* models is shown as well.